Neuroscience Letters 812 (2023) 137405

Contents lists available at ScienceDirect

Neuroscience Letters

journal homepage: www.elsevier.com/locate/neulet

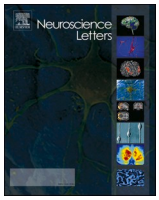

Evaluation of BCAS1-positive immature oligodendrocytes after cerebral ischemic stroke and SVD

Guanhua Jiang, Takashi Ayaki *, Takakuni Maki, Ken Yasuda, Daisuke Yoshii, Seiji Kaji, Ryosuke Takahashi

Department of Neurology, Kyoto University Graduate School of Medicine, Kyoto, Japan

ARTICLE INFO

Keywords:
Cerebral ischemia
Oligodendrocytes
OPCs
BCAS1
Immunohistochemistry

ABSTRACT

Ischemic cerebrovascular disease is an important cause of physical disability and dementia. Oligodendrocytes (OLGs), which differentiate from oligodendrocyte precursor cells (OPCs), are crucial for remyelination of the damaged brain and functional recovery. Breast carcinoma amplified sequence 1 (BCAS1) has recently been shown to be highly expressed in newly formed pre-myelinating oligodendrocytes (pre-mOLGs), while its expression level is reduced in mature OLGs. In this study, we analyzed BCAS1 expression by immunohistochemical analysis of human post-mortem brain tissue from six stroke patients (death within 2 months after stroke onset) and eight small vessel disease (SVD) patients. Control post-mortem brain tissue was from eight age-matched patients without any obvious central nervous system (CNS) pathology. The Olig2 expression in the area corresponding to the same section of the BCAS1-stained slice was analyzed to determine the total oligodendrocyte lineage. The percentage of differentiating OPCs in the oligodendrocyte lineage was calculated as the ratio of BCAS1+ to Olig2+ cells (BCAS1+/Olig2+). The stroke and SVD cases showed demyelination with decreased expression of myelin basic protein (MBP, a mature OLG marker). The stroke cases showed significantly increased numbers of early-stage BCAS1+ cells with an immature morphology and Olig2+ cells (pan-oligodendrocyte lineages) in the *peri*-infarct areas in both the cortex and white matter, but showed no increase in the number of late-stage BCAS1+ cells with a mature morphology. In contrast, the SVD cases showed no significant increase in Olig2+ and BCAS1+ cells. These results indicated that remyelination dysfunction could be attributed to insufficient maturation of OPCs in stroke and impaired recruitment of OPCs in SVD.

1. Introduction

Cerebrovascular disease is the primary cause of severe disability and the second-leading cause of death worldwide [1,2]. Ischemic stroke constitutes the greatest proportion of strokes, accounting for 75%-80% of all strokes [3].

Ischemic vascular injury damages the cortex and white matter of the brain. The pathological processes caused by ischemic vascular injury can be divided into acute (≤2 weeks), subacute (≤12 weeks), and chronic (13 weeks to months) stages [4,5]. During the acute phase, disruption of the blood–brain barrier and reperfusion through damaged cerebral blood vessels damages neurons and myelin, leading to cortex and white matter damage. The chronic phase, which involves more active apoptosis, angiogenesis, and remyelination, can last for weeks to months [6–8]. Persistent white matter damage and hindered recovery are crucial causes of post-stroke disability and cognitive impairment [9,10]. Ischemic stroke has been suggested to be related to small vessel disease (SVD), which encompasses several neurological processes that lead to reduced cerebral blood flow, chronic ischemia, and even acute stroke [11]. Although it may take years to progress, persistent hypoxia can result in demyelination and white matter damage [11,12].

Oligodendrocytes (OLGs) are the myelinating cells of the central

Abbreviations: BCAS1, Breast carcinoma amplified sequence 1; BDNF, Brain-derived neurotrophic factor; CNS, Central nervous system; CNTF, Ciliary neurotrophic factor; GFAP, Glial fibrillary acidic protein; HE, Hematoxylin and eosin; IHC, Immunohistochemistry; MBP, Myelin basic protein; OLG, Oligodendrocyte; OPC, Oligodendrocyte precursor cells; PDGF, Platelet-derived growth factor; PI, Peri-infarct; RA, Remote area; SVD, Small vessel disease; SVZ, Subventricular zone; VEGF, Vascular endothelial growth factor.

* Corresponding author at: Department of Neurology, Kyoto University Graduate School of Medicine, 54 Kawahara-cho, Shogoin, Sakyo-Ku, Kyoto 606-8507, Japan.

E-mail address: ayaki520@kuhp.kyoto-u.ac.jp (T. Ayaki).

https://doi.org/10.1016/j.neulet.2023.137405
Received 2 May 2023; Received in revised form 2 July 2023; Accepted 18 July 2023
Available online 20 July 2023

nervous system (CNS), which provide axons with the myelin sheath [13] and serve a variety of functions in the white matter of the brain [14]. OLGs do not have self-renewing capacity [15] and are vulnerable to oxidative stress, excitatory amino acids, and inflammatory cytokines [16]. Ischemic episodes are followed by the death of multiple OLGs within 3 h [17], and a consequent disruption of myelin architecture [18]. Similarly, SVD creates conditions of chronic hypoxia, which induces oxidative stress and inflammation, leading to OLG death in the white matter [11,12].

The repair of damaged OLGs is mediated by oligodendrogenesis, which includes recruitment, proliferation, and maturation processes. Oligodendrocyte precursor cells (OPCs), which are the immature form of OLGs, are locally present in the corpus callosum, the striatum, and the cortex and are derived from neural progenitor cells in the subventricular zone (SVZ) [19,20]. During stroke recovery, residual OPCs and OPCs generated from the SVZ are activated and proliferate and migrate to the *peri*-infarct area (penumbra), of which some mature into myelinating OLGs to compensate for the injured axons. Disruption of OLG maturation leads to the failure of remyelination, which hinders neurological recovery after stroke [21,22]. Some studies have suggested that the failure of remyelination in the SVD model could be related to an arrest in OPC maturation [23]. However, the detailed mechanisms underlying the disturbances in oligodendrogenesis during stroke and SVD recovery remain unclear.

Breast carcinoma amplified sequence 1 (BCAS1) was originally identified as a messenger ribonucleic acid (mRNA) amplified in human cancer cell lines [24] and has been shown to be highly expressed in OLGs [25]. Although the precise function of BCAS1 remains unknown, the expression of BCAS1 was shown to be upregulated in the cerebral cortex 3 weeks after birth in a mouse model, similar to myelin basic protein (MBP) expression, and BCAS1 knockout mice showed reduced anxiety and schizophrenia-like behavioral abnormalities as well as mild hypomyelination [26,27]. BCAS1 is also known to be highly expressed in premyelinating OLGs (pre-mOLGs), and its expression is reduced in mature oligodendrocytes [28].

In this study, we investigated whether BCAS1 could serve as a marker of oligodendrogenesis after ischemic brain injury. To this end, we used BCAS1 immunohistochemistry to examine the expression of BCAS1 in human brains showing cerebral infarction and SVD and explored the changes in pre-mOLGs in the OPC population after ischemic stroke and SVD. Our results showed that after ischemic stroke, early-stage BCAS1+ cells and Olig2+ cells, but not late-stage BCAS1+ cells, were significantly increased in the *peri*-infarct demyelinating areas, which may indicate increased recruitment of OPCs without proper maturation into mOLGs. In contrast, the SVD group did not show an increase in Olig2+ and BCAS1+ cells, indicating impaired recruitment of OPCs to demyelinating lesions in SVD.

2. Methods

2.1. Human tissue sample collection

CNS tissue was obtained from the archives of the Institute of Neuropathology at Kyoto University. This study was approved by the local ethics committee (R1038). For the control group, frontal or temporal cortex and white matter samples were obtained from seven autopsy cases without obvious ischemic history and pathology. SVD was diagnosed on the basis of previously published criteria [29,30]. The majority of the eight SVD samples were obtained from the temporal lobe of patients showing ischemic changes. For stroke samples, the location of the stroke was relatively variable, and included the frontal, temporal, parietal, and occipital lobes and the motor area. In the stroke group, the *peri*-infarct area was selected randomly within the zone bordering the infarct core, and the remote area was defined as the region farther than 1.0 cm away from the infarction. The duration of the stroke process was 1–2 months. Most patients experience systemic ischemia due to respiratory failure before death. The age ranges of the stroke patients, SVD patients, and normally aged control participants were 73–93 years, 70–90 years, and 68–95 years, respectively. For the stroke group, disease duration (time before death) ranged from 1 to 2 months. Detailed clinical information is presented in Table 1.

2.2. Immunohistochemistry

Paraffin-embedded tissue sections (6 μm) were deparaffinized, stained with hematoxylin and eosin (HE) or Klüver-Barrera (KB), and subjected to immunohistochemistry (IHC) in accordance with standard procedures. The following primary antibodies were used: For activated astrocytes and microglia, rabbit anti-glial fibrillary acidic protein (GFAP) antibody (ab7260, 1:200; Abcam), and mouse anti-CD68 antibody (M0814, 1:100; Dako) were applied, respectively. Demyelination of the brain samples was confirmed using a rabbit anti-MBP antibody (PD004, 1:200; MBL). For BCAS1 specificity, double-labeling IHC was performed using a mouse anti-BCAS1 antibody (sc-136342, 1:500; Santa Cruz) and a rabbit anti-Olig2 antibody (JP18953, 1:300; IBL International), rabbit anti-NG2 antibody (AB5320, 1:100; Merck Millipore), or rabbit anti-CC1 antibody (OP80, 1:50; Merck Millipore). To demonstrate that the BCAS1+ cells were from the oligodendroglial lineage, two consecutive brain samples from the same autopsy case were stained with either mouse anti-BCAS1 antibody (sc-136342, 1:500; Santa Cruz) or rabbit anti-Olig2 antibody (JP18953, 1:300; IBL International). Antibody binding was visualized using biotinylated secondary antibodies (414151F; Histofine), peroxidase-conjugated avidin, and diaminobenzidine (415194F; Histofine). Double-labeling immunohistochemistry was performed by combining diaminobenzidine and Fast Red by using an alkaline phosphatase-conjugated secondary antibody (MP-5402; Vector).

2.3. Morphometric analysis

Immunopositive cell densities in each immunohistopathological tissue sample were determined using a 10 × 10 ocular morphometric grid (at 200 × magnification) (Olympus, Japan), and the results were expressed as cells/mm^2. BCAS1+ cells were manually counted using the ImageJ software (ver. 1.46r, NIH). All Olig2 antibody stained sections were counterstained with hematoxylin. The percentage of Olig2+ OLG lineage cells was counted automatically using ImageJ as Olig2+ cell numbers in the total hematoxylin-stained cell nuclei. To determine the percentage of BCAS1+ cells in OLG lineage cells, the total number of Olig2+ cells was counted in the same area as BCAS1-stained sections from two consecutive brain samples. MBP quantification was also performed using the ImageJ software (ver. 1.46r, NIH). MBP images were processed with calibration and threshholding, and the ratio of MBP-positive area was calculated as the area of thresholded image divided by the area of full image.

2.4. Statistical analysis

All statistical analyses were performed using GraphPad Prism 8 software (GraphPad Software). Normal distribution was tested using the Kolmogorov–Smirnov test with Dallal–Wilkinson-Lillie for p-values. The Mann–Whitney *U* test was used to compare the two groups. Kruskal–Wallis one-way analysis of variance with Dunn's multiple-comparison test was performed to compare three or more groups. Data were presented as mean ± SEM, unless stated otherwise. The asterisks corresponded to p-values < 0.05 (*), <0.01 (**), and < 0.001 (***).

Table 1
Clinical and pathological Information of the subjects.

	Gender	Age of death (y)	Disease Duration (m)	Clinical diagnosis	Area	Cause of death
Stroke group (n = 6)	Female	74	1.5 months	Cerebral infarction	Occipital lobe	NA
	Male	73	1.5 months	Cerebral infarction	Frontal lobe	Respiratory failure
	Male	84	NA	Multiple cerebral infarction	Motor area	NA
	Male	89	2 months	Cerebral infarction	Parietal lobe	Multiorgan failure
	Female	93	1 month	Cerebral infarction	Parietal lobe	Apnea
	Male	84	2 months	Cerebral infarction	Occipital lobe	Liver failure
Control group (n = 7)	Female	71	NA	Carcinomatous meningitis	Temporal lobe	NA
	Female	68	NA	Senile change	Motor area	NA
	Male	72	NA	NA	Motor area	Respiratory failure
	Male	92	NA	NA	Frontal lobe	Heart failure, kidney failure
	Male	95	NA	NA	Frontal lobe	DIC
	Male	76	NA	Parkinson's disease	Motor area	DIC
	Female	69	NA	Dementia with Lewy bodies	Motor area	Pneumonia
SVD group (n = 8)	Male	90	NA	Ischemic leukoencephalopathy	Temporal lobe	Heart failure
	Female	77	4 months	Ischemic changes, Alzheimer type of degeneration	Temporal lobe	Pneumonia
	Male	70	12 months	Superficial hemosiderosis, multiple lacunar infarction	Temporal lobe	Pneumonia
	Female	82	12 months	Multiple lacunar infarction in basal ganglia	Temporal lobe	Pneumonia
	Male	82	22 months	Binswanger's disease	Frontal lobe	Pneumonia
	Male	85	21 months	Binswanger's disease	Temporal lobe	Pneumonia
	Female	86	23 months	Binswanger's disease	Temporal lobe	Pneumonia
	Female	76	14 months	Binswanger's disease	Temporal lobe	Sepsis

Abbreviation: NA: Not available; DIC: Disseminated intravascular coagulation.

3. Results

3.1. Ischemic cell changes and demyelination were confirmed in stroke and SVD cases

Detailed clinical information is presented in Table 1. The age range of the stroke patients, SVD patients, and control individuals was 73–93 years, 70–90 years, and 68–95 years, respectively (Table 1). The time from stroke onset to autopsy was 1–2 months.

Ischemic cell changes and demyelination were observed in both stroke and SVD cases (Fig. 1). KB (Fig. 1A) and HE (Fig. 1B) staining revealed ischemic changes in the stroke patients. Severe neuronal death and axonal loss were observed in the core of the ischemic territory, with GFAP + astrocytes (Fig. 1C) and clustered CD68 + microglia (Fig. 1D) in the *peri*-infarct areas. In stroke cases, the remote area was defined as an area farther than 1.0 cm away from the infarction without any evident ischemia on KB and HE staining. MBP staining further confirmed that both stroke and SVD patients showed areas of reduced myelin staining. In the *peri*-infarct areas of stroke patients, gray and white matter showed decreased MBP immunoreactivity (Fig. 1E, F). The MBP + area also decreased in the remote areas in the stroke cases (Fig. 1G, H). In the SVD cases, the white matter showed decreased MBP immunoreactivity (Fig. 1I, H, N). The results of NG2 + single staining are shown in supplementary figures (Supplementary Fig. 1A-D).

3.2. The BCAS1 antibody was a specific marker for differentiating OPCs/OLGs in the control and stroke groups

Cells labeled for BCAS1 were observed in all samples in the stroke, SVD, and control groups. We evaluated the antibody specificity for premOLGs by using alkaline phosphatase double staining. Almost all BCAS1+ cells were co-labeled with Olig2 (Fig. 2A, B), but the labeling rarely overlapped with that for NG2 (Fig. 2C, D) and CC1 antibodies (Fig. 2E, F).

Two different morphologies of BCAS1+ cells were identified in all the cases. One BCAS1+ cell population showed a smaller nucleus and cytoplasm and extended large branches (Fig. 2H, arrow). Another population consisted of rounder cells with almost no branched processes in the cortex (Fig. 2H, arrowheads) or white matter (Fig. 2J, arrowheads). Previous reports have suggested that BCAS1 staining is localized to the cell cytoplasm and shows different morphologies during maturation. In the early stages of maturation, BCAS1+ cells appear rounder, with almost no branched processes, and have a larger nucleus, indicating a more immature OPC-like morphology. In the later stage, the cells show a smaller nucleus and cytoplasm and extended large myelin-like membrane sheets [28,31]. On the basis of these reports, the BCAS1+ cells with branches (Fig. 2H, arrow) were classified as "late-stage BCAS1+ cells" and the BCAS1+ cells without branches (Fig. 2H, J, arrowheads) are classified as "early-stage BCAS1+ cells.".

In the aged cerebral cortex of the control group, the density of early-stage BCAS1+ cells was approximately 12 ± 2.6 cells/mm^2, which was almost six times higher than that of the late-stage cells (2.3 ± 0.4 cells/mm^2) (Fig. 2K). Moreover, in the white matter, the density of early-stage BCAS1+ cells was approximately 5.3 ± 1.8 cells/mm^2, while the density of late-stage cells was approximately the same as that in the cortex (1.1 ± 0.17 cells/mm^2) (Fig. 2L). These measurements of the density of BCAS1+ cells were consistent with those reported in a previous study [28].

3.3. Early-stage BCAS1+ cells were significantly increased in the peri-infarct areas and remote areas of the stroke group

We then investigated the distribution of BCAS1+ cells in the stroke (Fig. 3 A-G) and SVD groups (Fig. 3H, J). BCAS1+ cells were abundantly observed in the *peri*-infarct areas (Fig. 3A-D). The early-stage BCAS1+ cells were significantly greater in number and concentrated around the *peri*-infarct areas (Fig. 3 J), while the late-stage BCAS1+ cells were difficult to identify (2.1 ± 0.56 cells/mm^2 in the cortex and 2.1 ± 0.73 cells/mm^2 in white matter; Fig. 3K).

The number of early-stage BCAS1+ cells in the *peri*-infarct and remote areas showed wide variations among samples, ranging from 51 to 226 cells/mm^2 in the cortex and 63 to 616 cells/mm^2 in the white matter in the *peri*-infarct areas, and from 5.1 to 177 cells/mm^2 in the cortex and 5.1 to 690 cells/mm^2 in the white matter in the remote areas. Despite the large variance within stroke cases, which may be attributable to differences in stroke severity and stages, the increase in the number of early-stage BCAS1+ cells in the stroke group was statistically significant (Fig. 3J, K). Quantification data showed that the number of early-stage cells had increased 58-fold in the white matter (309 ± 58 cells/mm^2; $p < 0.0001$) and 13-fold in the cortex (158 ± 24 cells/mm^2, $p < 0.0001$) in comparison with the control samples (Fig. 3J).

In the remote areas of the stroke samples, early-stage BCAS1+ cells showed similar changes as in the *peri*-infarct areas, with 26-fold and 6-fold increments in the white matter and cortex, respectively (Fig. 3F,

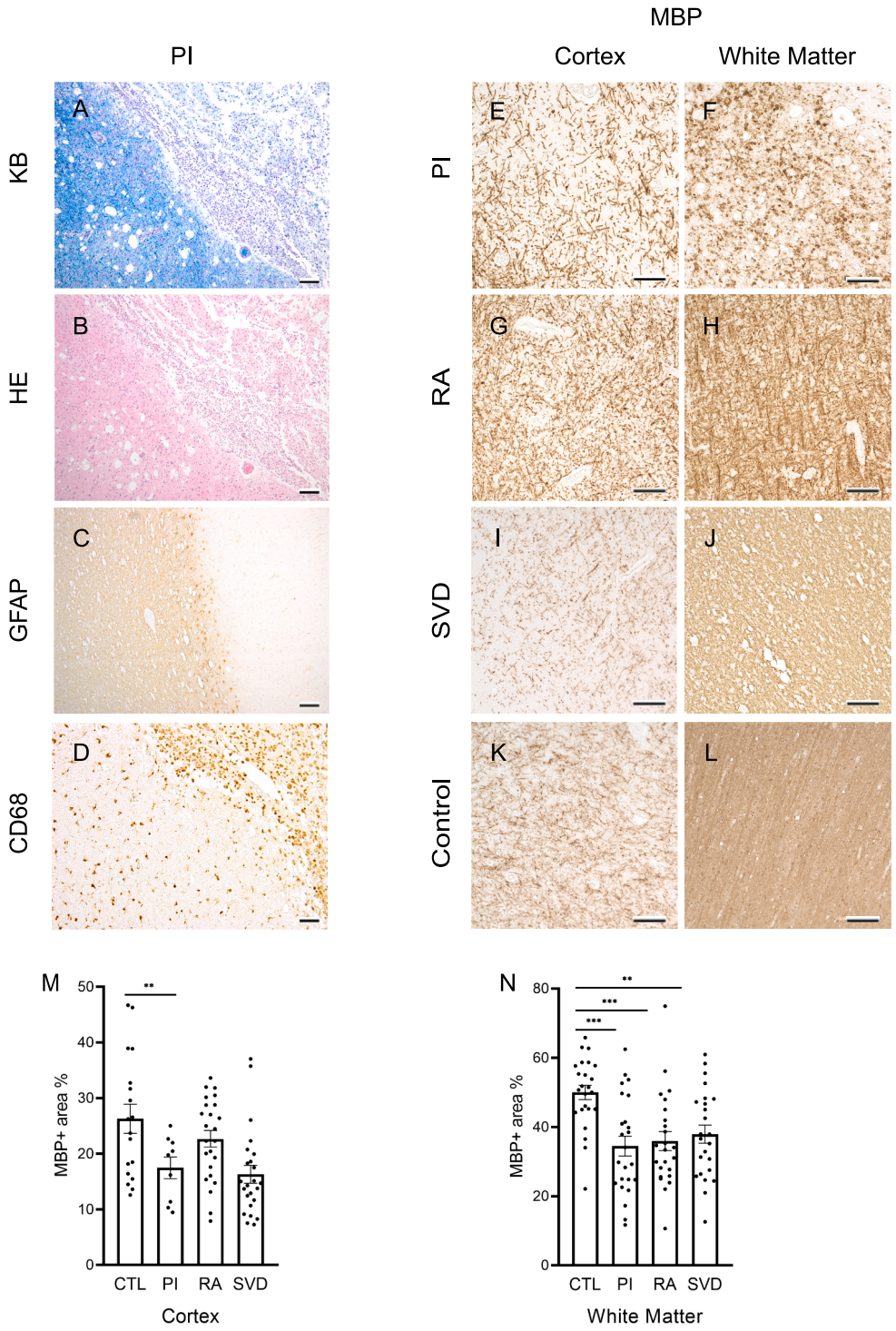

Fig. 1. Ischemic cell changes and demyelination were confirmed in the stroke and SVD cases. (A-D) Representative images of KB, HE, GFAP, and CD68 staining in the *peri*-infarct area of stroke. (E-L) MBP immunohistochemistry of the penumbra (E, F) and remote area of a stroke case (G, H) and an SVD case (I, J), and the occipital lobe of a control case (K, L). (M, N) Quantification of the MBP + mean gray area in the white matter and cortex in each group. PI, *peri*-ischemic area; RA, remote area. (Kruskal–Wallis test with Dunn's post-hoc test, *p < 0.05, **p < 0.01, ***p < 0.001, ****p < 0.0001. n = 5–8, with three sections per case. Quantitative data are presented as the mean ± SEM. Scale bar = 100 μm).

G; $p < 0.001$) in comparison with the control samples. However, late-stage BCAS + cells showed no significant changes in comparison with the control group. In contrast to the findings for the stroke group, the SVD group showed no significant change in the early- and late-stage BCAS1+ cell numbers (Fig. 3H, I).

3.4. *Percentage of BCAS1+ cells in the Olig2 lineage in the ischemic brain*

To determine the ratio of BCAS1+ cells in the total OLGs, we investigated Olig2+ cells in all cell types (Fig. 4) and the percentage of BCAS1+ cells in the total Olig2 lineage in each group (Fig. 5). First, we confirmed an increase in Olig2+ cells in stroke patients (Fig. 4. C, D). The percentage of Olig2+ OLGs (% of Olig2 in Fig. 4 I, J) was counted as the number of Olig2+ cells in the total hematoxylin-stained cell nuclei. In the *peri*-infarct areas, the percentage of Olig2+ cells among all cell types was 24%±4.3% in the cortex and 54%±8% in the white matter; both were greater than the corresponding values in the control group (8.7%±1.2% in the cortex, 29%±7.6% in the white matter). Although the percentage of Olig2+ cells also increased in the remote area of the white matter, the intergroup difference for this increase was not

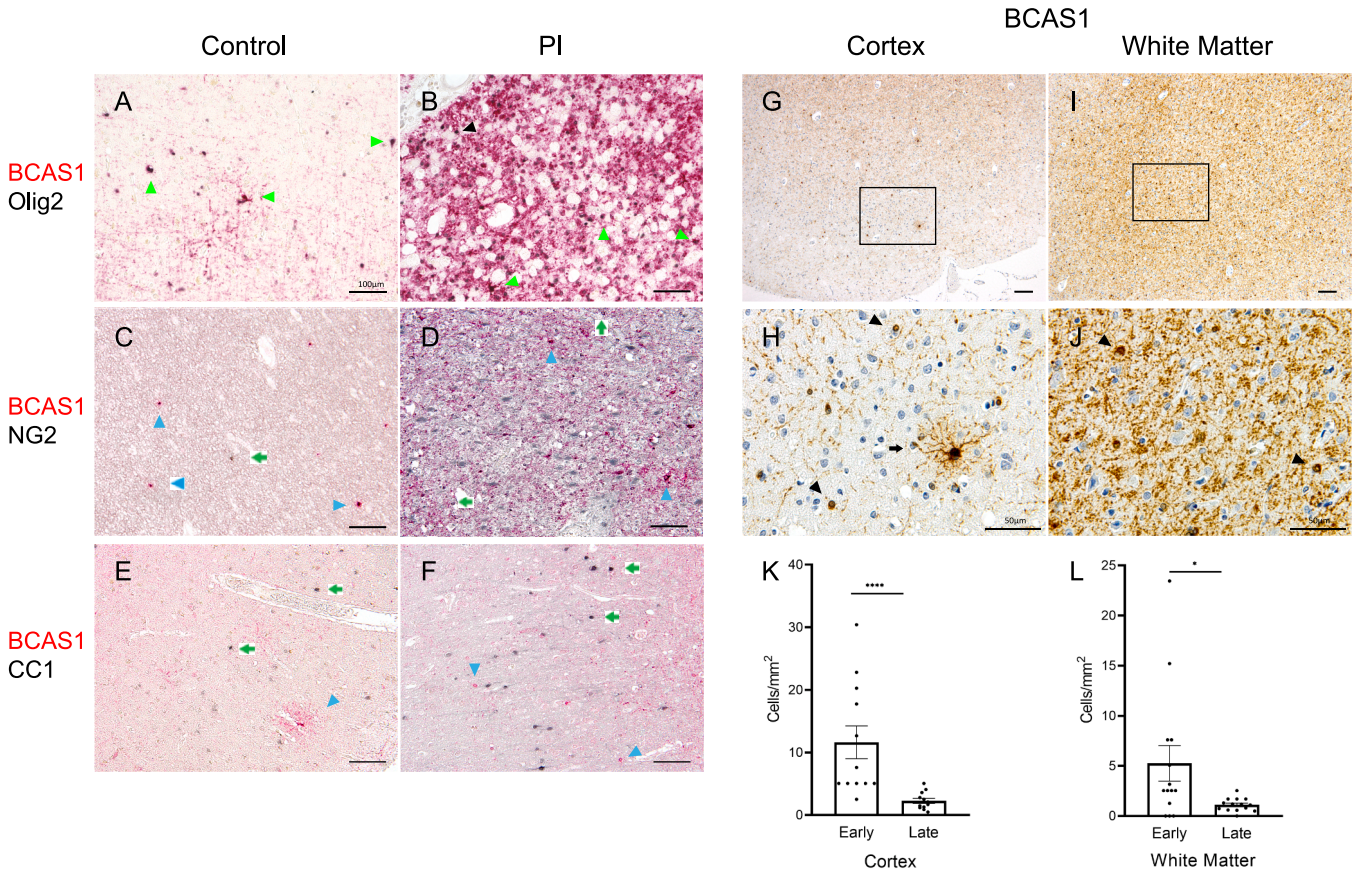

Fig. 2. BCAS1 antibody specificity and different morphologies of BCAS1+ cells. (A-F) Alkaline phosphatase double-staining images of BCAS1 (red) with Olig2 (black), NG2 (black), and CC1 (black) in the control and *peri*-infarct areas. Almost all BCAS1+ cells were co-labeled with Olig2 (A, B). BCAS1+/Olig2+ cells (Green arrowhead) and BCAS1-/Olig2+ cells (black arrowheads) are shown (A, B). BCAS1 rarely merged with NG2 (C, D) or CC1 (E, F). Double staining shows BCAS1+/NG2- cells (blue arrowheads in C, D), BCAS1-/NG2 + cells (green arrows in C, D), BCAS1+/CC1- cells (blue arrowheads in E, F), and BCAS1-/CC1 + cells (green arrows in E, F). (G-J) Representative images of BCAS1+ cells in the frontal cortex (G) and the white matter (J). Magnified images of (G) and (I) are shown in (H) and (J), respectively. Early-stage BCAS1+ cells (black arrowhead in H and J) appeared rounder, with almost no branched processes, and had a large nucleus, which showed a more OPC-like morphology. Late-stage BCAS1+ cells (black arrow in H) extended into large myelin-like membrane sheets in culture (K, L). Quantification of the early and late stages of BCAS1+ cell density in the white matter and cortex. (Unpaired Mann–Whitney test, *p < 0.05, ****p < 0.0001). n = 6, two sections per case. Quantitative data are presented as the mean ± SEM. Scale bars: A-G, I = 100 μm; H, J = 50 μm).

significant (p = 0.1995. Fig. 4I, J) (see Fig. 6).

We then quantified the number of BCAS1+ cells in the same region as Olig2 to obtain the percentage of BCAS1+ cells in the total Olig2 lineage (BCAS1+%) (Fig. 5). In the white matter, the BCAS1+% increased by 22.4% in the penumbra (p < 0.0001; Fig. 5T). However, the increase in BCAS1+% in remote areas of the white matter did not reach significance (p = 0.2981). Although the cortex BCAS1+/Olig2+ ratio was increased in SVD, it was most likely due to the decrease in the number of Olig2+ cells, since the findings showed a 12.42% (p = 0.0817) reduction in Olig2+ cells in the SVD cortex (Fig. 4I). As for gender differences, although the current data did not provide significant evidence (Supplementary Fig. 2), further analysis in future studies might reveal some new perspectives.

These results (Fig. 5 S, T) suggest that active OPC recruitment (i.e., proliferation and/or migration) without complete maturation was induced in the *peri*-infarct areas in stroke cases. However, neither OLG lineages nor the ratio of cortex BCAS1+/Olig2+ increased in the SVD group, suggesting that demyelination and OLG death under mild hypoxia could not trigger OPC recruitment.

4. Discussion

In the present study, the morphological characteristics of BCAS1+ cells showed a typical pattern described in previous reports [28]. During the early stage of differentiation, BCAS1+ cells appeared rounder, with almost no branched processes, and had a larger nucleus, showing a more OPC-like morphology. In the later stage, the cells showed a smaller nucleus and cytoplasm and extended large myelin-like membrane sheets in culture. BCAS1 immunoreactivity was first observed in the soma and later appeared in newly formed non-compacted myelin sheaths and diminished in compacted myelin-like membrane sheets [2832]. Although the precise function of BCAS1 remains unclear, it has been thought to be involved in the development of white matter [26]. In our study, pre-OLGs showed a BCAS1-positive status during oligodendrogenesis, while immature OPCs and mature OLGs did not show positive results for BCAS1.

Both ischemic stroke and SVD involve reduced blood flow to the brain and the creation of an oxidative and proinflammatory environment that causes demyelination and remyelination. In the present study, while the MBP density was decreased in both the stroke and SVD groups, the BCAS1+ OLGs showed different patterns between the stroke and SVD groups. Although the stroke group showed an increased density of Olig2 and early-stage BCAS1+ cells, the SVD group did not show an increase in Olig2 and BCAS1+ cells.

The number of early-stage BCAS1+ cells was significantly higher in the stroke group in the present study. These results indicate that OPCs are abundantly recruited during acute ischemic conditions. Moreover, the total number of OLG lineages in the *peri*-infarct areas was increased

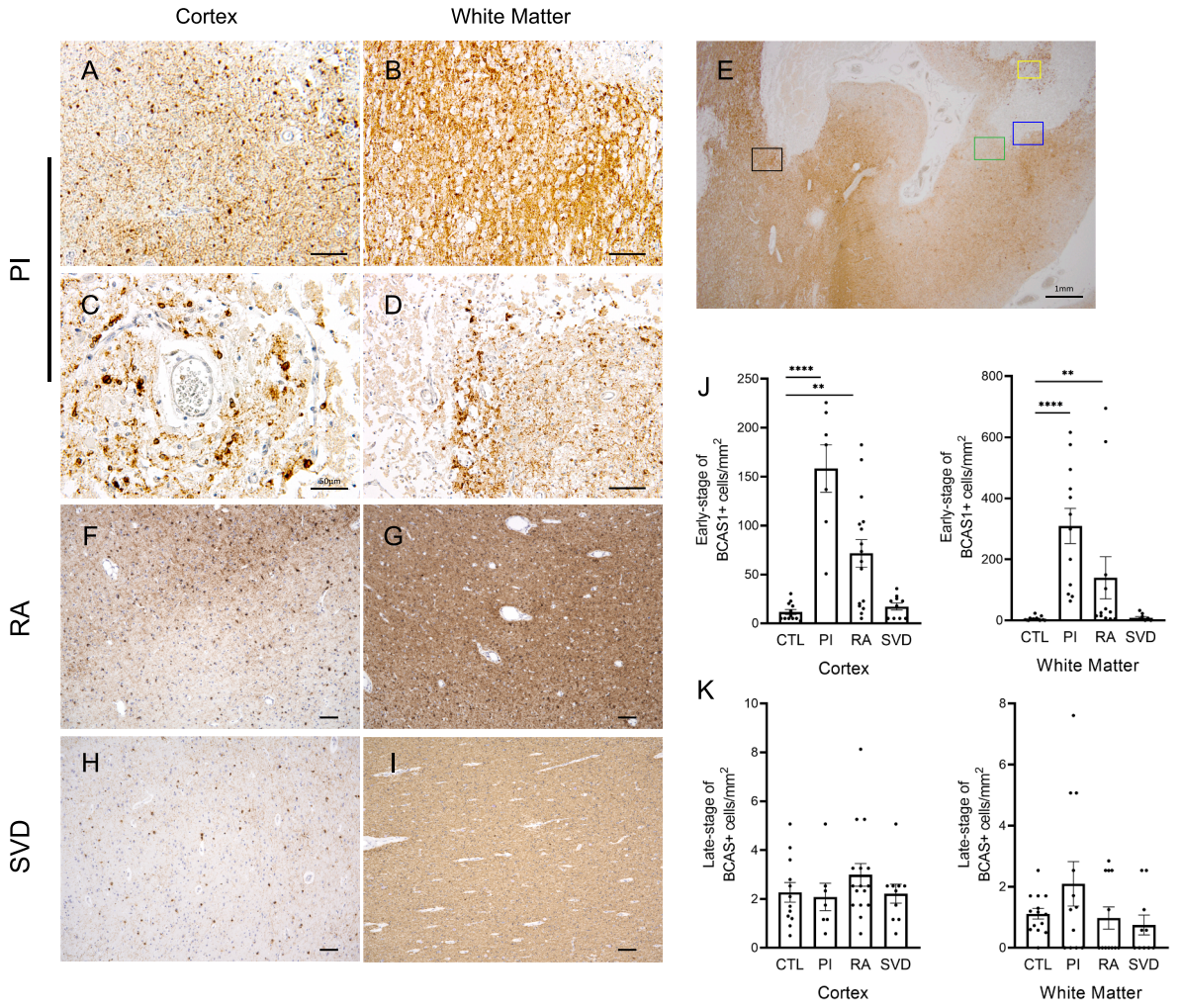

Fig. 3. Early-stage BCAS1-positive cells are significantly increased in the *peri*-infarct area and remote area in the stroke group. (A-D) Magnified images of BCAS1 immunohistochemistry in the *peri*-infarct area (E). Fig. 3 (A-D) represent the areas in the green (A), black (B), yellow (C), and blue (D) box, respectively. (F, G) BCAS1+ cells are increased in the remote area of the stroke case (F, G). (H, I) No significant changes in BCAS1+ cells were seen in the SVD cases. (J, K) Quantification of BCAS1+ cell density in the early (J) and late stages (K) in the cortex and white matter. PI, *peri*-ischemic area; RA, remote area (Kruskal–Wallis test with Dunn's post-hoc test, *p < 0.05, **p < 0.01, ***p < 0.001, ****p < 0.0001; n = 5–8, two sections per case. Quantitative data are presented as the mean ± SEM. Scale bars: A, B, D-I = 100 μm; C = 50 μm).

in both the cortex and white matter, indicating the migration and/or proliferation of OPCs in the lesion area. Cerebral ischemic stroke produces severe neuronal death and more sustained hypoxia and inflammation with the secretion of trophic factors and proinflammatory signaling proteins (cytokines and chemokines) from reactive astrocytes, macrophages, microglia, and cerebral endothelial cells [33]. In particular, trophic factors are essential since they promote OPC proliferation, migration, and differentiation. For example, astrocytes express basic fibroblast growth factor (bFGF) and endothelial cell-derived vascular endothelial growth factor (VEGF), which can also induce OPC migration [34,35]. Platelet-derived growth factor (PDGF), brain-derived neurotrophic factor (BDNF), and insulin-like growth factor-I (IGF- l) from astrocytes, endothelial cells, and microglia, respectively, can promote OPC proliferation [36–39]. Astrocyte-derived BDNF, astrocytes, and microglia-derived ciliary neurotrophic factor (CNTF) can promote OPC differentiation [40]. Under the effects of these tropic factors, residual OPCs and OPCs generated from the SVZ undergo activation, proliferation, and migration to the *peri*-infarct area [15,41]. Thus, these tropic factors can be reasonably assumed to promote the recruitment of OPCs in our study.

In contrast to the findings for the stroke group, the density of Olig2 and BCAS1+ cells did not increase in the SVD group in our study. Since SVD does not present with massive acute infarction unlike stroke, SVD cases may not show the expression of trophic factors that trigger OPC proliferation and migration. One study using a rat model of chronic hypoxia reported the expression of hypoxia-inducible factor-1α (HIF-1α), a transcription factor that regulates adaptive responses to oxygen deficiency, and the HIF-1 target genes, glucose transporter-1 (GLUT-1), and VEGF [42,43]. However, during prolonged hypoxia, HIF-1α expression was significantly elevated for 14 days and returned to near baseline levels by 21 days despite the continuous low arterial oxygen tension [44]. On the other hand, acute hypoxia causes a fluctuating yet continuous increase until 8 days in the expression of HIF-1α as well as its target genes, glucose transporter-1, and VEGF, which has been proven to promote OPC migration [45]. Further investigation is needed to clarify the difference between hypoxic gradients and changes over time after stroke and chronic hypoxia in SVD, and the underlying mechanisms that affect OPC behavior.

Although the number of BCAS1+ cells among OLlG2-positive cells at the white matter of *peri*-infarct areas of stroke increased, only some of the recruited OPCs could differentiate into mature myelinating OLGs in the stroke cases in the present study. Several factors can affect OLG

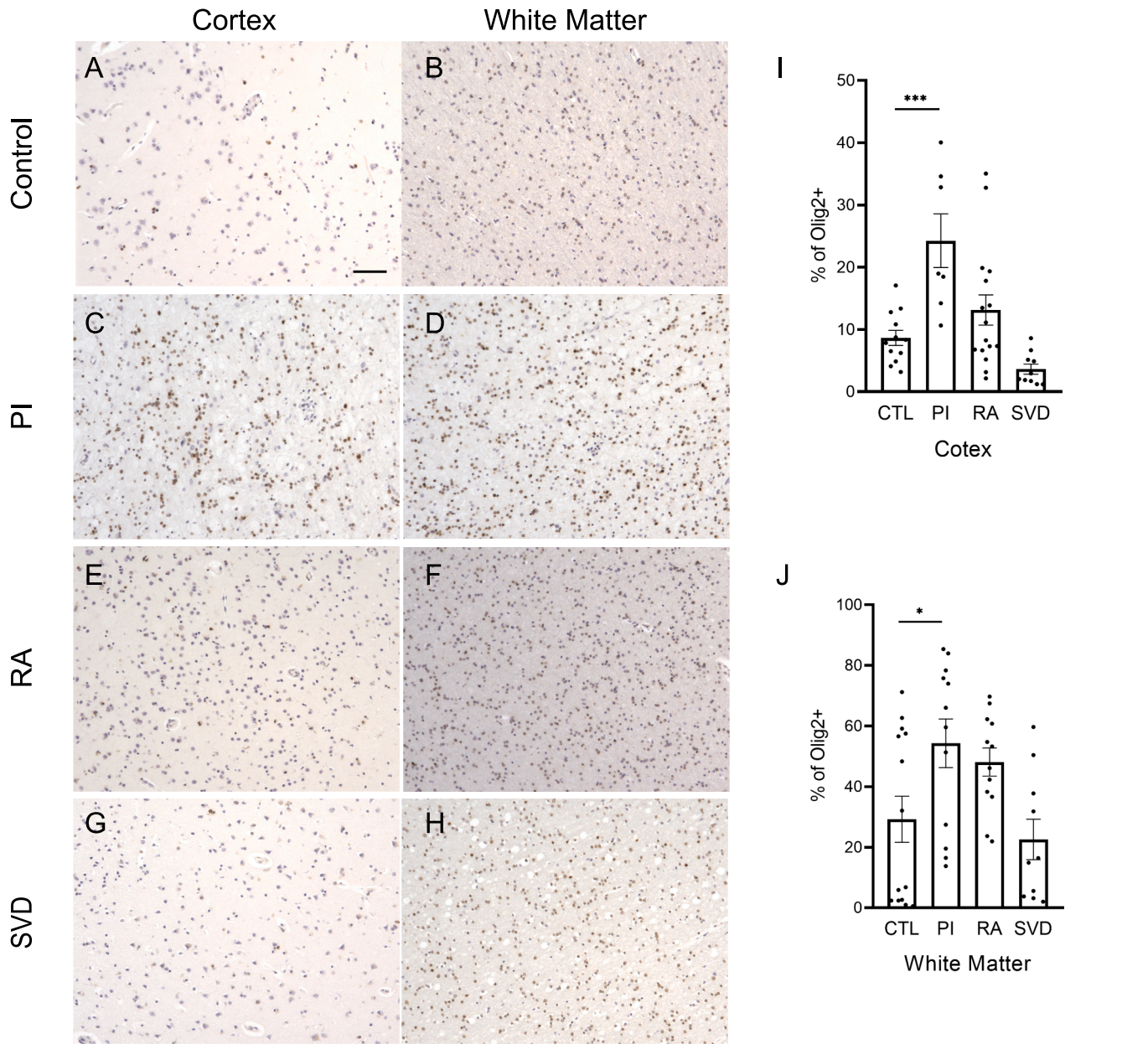

Fig. 4. Olig2+ cells are increased at *peri*-infarct area. Representative images of Olig2 immunohistochemistry in the control group (A, B), *peri*-infarct area (C, D), remote area (E, F), and SVD groups (G, H). Quantification of Olig2+ cell percentage in the total hematoxylin-stained cell nuclei in the cortex (I) and white matter (J). PI, *peri*-ischemic area; RA, remote area (n = 5–8, two sections per case). Kruskal–Wallis test with Dunn's post-hoc test, *p < 0.05, **p < 0.01, ***p < 0.001, ****p < 0.0001. Quantitative data are presented as the mean ± SEM. Scale bar = 100 μm).

maturation under ischemia. The primary factor influencing maturation is apoptosis of OPCs under ischemic conditions. In a neonatal rat model of hypoxic-ischemic injury, O4-positive late OPCs were decreased via apoptotic cell death [46], and it is reasonable to assume that most early-stage BCAS1+ cells undergo apoptosis due to their vulnerability to hypoxia, with only a small percentage of these cells differentiating into late-stage BCAS1+ cells. Second, BCAS1+ cells eventually die because of the loss of axons, although late-stage BCAS1+ cells show increased resistance to cell death due to oxidative stress. The massive axon loss in stroke limited the neuronal activity for these cells to differentiate into functional myelinating OLGs since pre-mOLGs have a limited time before being connected with axons. Third, maturation arrest can be induced by various factors that inhibit OPC differentiation in cell-autonomous and non-cell-autonomous manners [36].

Our study also showed that the SVD group lacked mature OLGs. Several factors can influence the maturation of OLGs under chronic ischemia. One possible explanation is the loss of maturation factors during the chronic period. Some growth factors such as astrocyte-derived BDNF have been proven to be crucial for OPC differentiation [40,47] in addition to OPC proliferation and migration, as mentioned above. BDNF levels increased within 24 h after acute stroke onset and returned to normal at 8 days. During the early and late stages of stroke, neurons, endothelial cells, microglial cells, and astrocytes in ischemic lesions were primarily responsible for BDNF production [48]. The differentiation arrest of resident OPCs in SVD may be partially related to the lack of BDNF. Under chronic hypoxia, BDNF levels gradually decreased, and the ratio of GFAP/BDNF double-positive cells decreased in a time-dependent manner, although the number of GFAP-positive astrocytes increased [49,50]. Another possible explanation is the quiescent state of resident OPCs, which has been reported in

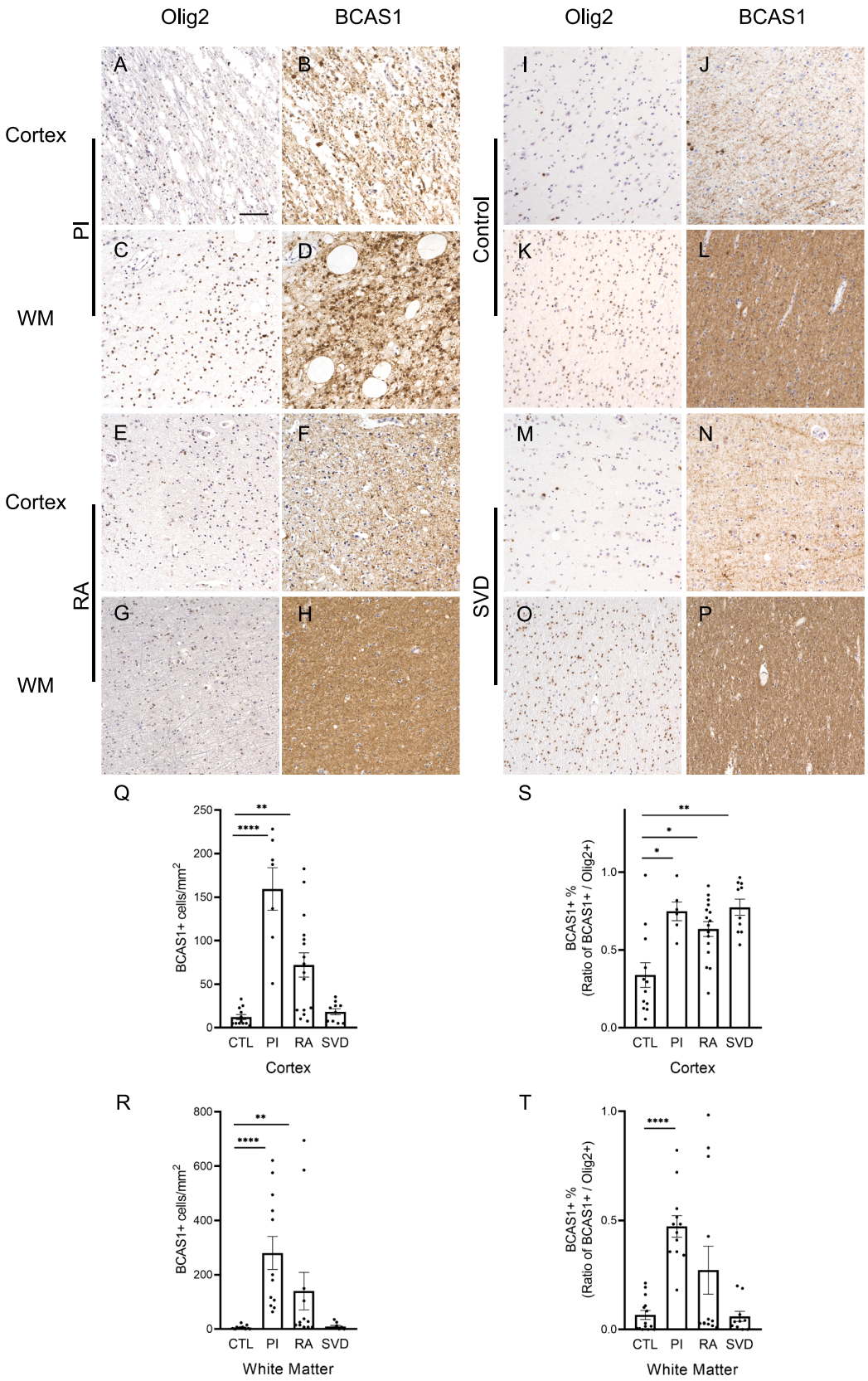

Fig. 5. Percentage of BCAS1+ cells in oligodendrocyte lineage. The same region from two consecutive brain slices stained with Olig2+ (A, C, E, G, I, K, M, O) and BCAS1+ (B, D, F, H, J, L, N, P) antibodies in the *peri*-infarct (A-D), remote (E-H), control (I-L), and SVD (M−P) areas. Quantification of BCAS1+ cell density (Q, R) and percentage of BCAS1+ cells in Olig2+ cells (S, T) in the white matter and cortex. (n = 5–8, two sections per case). PI, *peri*-ischemic area; RA, remote area. (Kruskal–Wallis test with Dunn's post-hoc test, *p < 0.05, **p < 0.01, ***p < 0.001, ****p < 0.0001. Quantitative data are presented as the mean ± SEM. Scale bar = 100 μm).

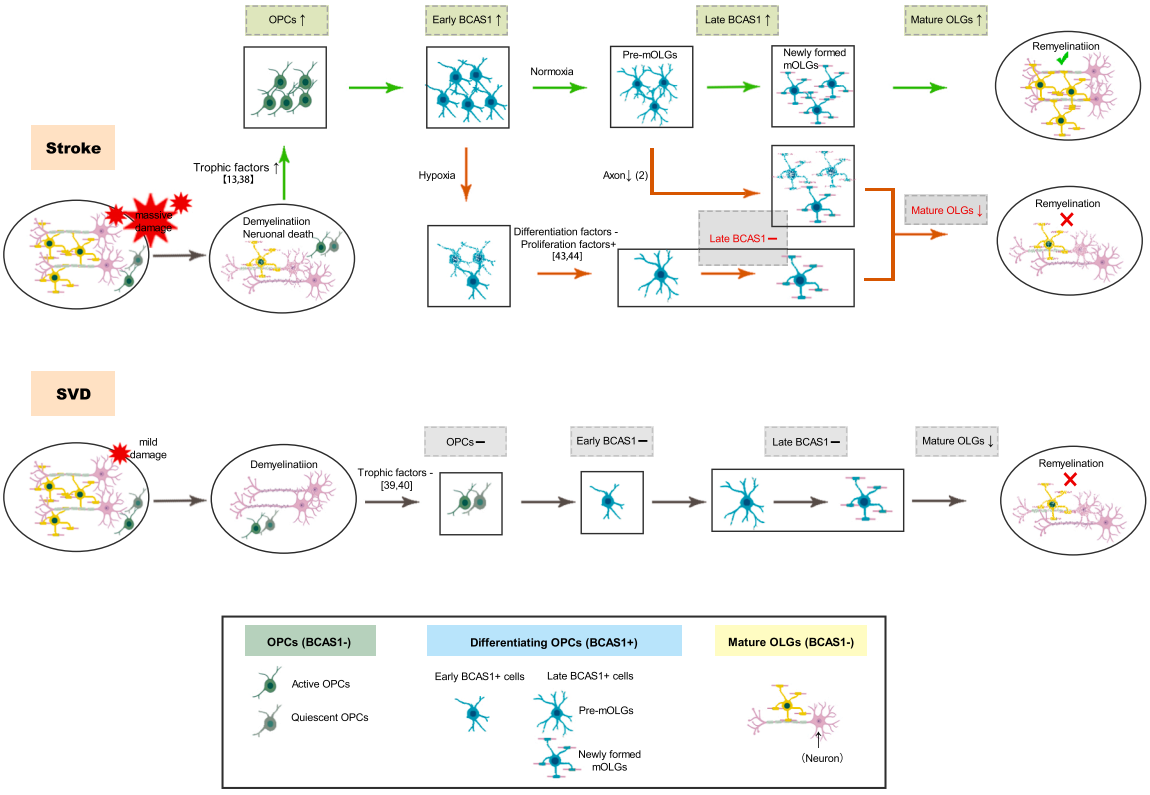

Fig. 6. Schematic representation of the presumed remyelinating process in normoxia and acute and chronic ischemia. After acute ischemia, under the effect of trophic factors (recruitment and differentiation factors), residual and recruited OPCs are activated, proliferate, migrate to the *peri*-infarct area, and differentiate into early-stage BCAS1+ cells [13,37]. Under normoxia, early-stage BCAS1+ cells eventually mature into functional oligodendrocytes and undergo complete remyelination. However, under ischemic stroke, most early-stage BCAS1+ cells fail to mature, probably because of their vulnerability to hypoxia, loss of axons, lack of sustained differentiation factors, or inhibition of overexpressed proliferation factors during acute ischemia [42,43]. In SVD, since some resident OPCs are in a quiescent state and lose their ability to proliferate and differentiate efficiently without appropriate recruitment and differentiation factors, full remyelination is hindered [38,39].

inflammatory and aging conditions. For instance, OPCs in multiple sclerosis lesions are classified as quiescent cells that lost the ability to proliferate and differentiate efficiently [51]. Insufficient proliferation and prolonged quiescence of resident OPCs may lead to remyelination failure in SVD [52–54].

The limitations of the present study are related to the limited number of stroke patients, who showed heterogeneity in injury severity, area, and complications. Moreover, the preservation of gray and white matter in these patients may not be as intact as in control samples, which may have influenced OPC behavior. Furthermore, since aging is reported to be related to the differentiation capability of OPCs [55,56], BCAS1 expression in young human stroke samples may need to be evaluated. A larger patient cohort or more controllable animal stroke models may be warranted in the future.

In conclusion, while stroke cases showed impaired maturation of early-stage BCAS1+ cells into late-stage BCAS1+ cells, SVD cases showed impaired recruitment of OPCs. On the basis of these peculiarities of OPC dynamics in stroke and SVD, promoting further maturation of differentiating OPCs or relieving maturation arrest is a possible target for remyelination and functional recovery after stroke, whereas it may be more important to enhance OPC recruitment for SVD.

Funding

This work was supported by MEXT KAKENHI (grant number: 19 K16277).

CRediT authorship contribution statement

Guanhua Jiang: Writing – original draft, Software, Formal analysis, Investigation, Data curation, Visualization. **Takashi Ayaki:** Writing – review & editing, Conceptualization, Validation, Resources, Data curation, Funding acquisition. **Takakuni Maki:** Resources, Supervision, Funding acquisition. **Ken Yasuda:** Methodology. **Daisuke Yoshii:** Writing – review & editing. **Seiji Kaji:** Conceptualization, Methodology. **Ryosuke Takahashi:** Supervision, Project administration, Funding acquisition.

Declaration of Competing Interest

The authors declare that they have no known competing financial interests or personal relationships that could have appeared to influence the work reported in this paper.

Data availability

Data will be made available on request.

Appendix A. Supplementary data

Supplementary data to this article can be found online at https://doi.org/10.1016/j.neulet.2023.137405.

References

[1] R. Lozano, et al., Global and regional mortality from 235 causes of death for 20 age groups in 1990 and 2010: A systematic analysis for the Global Burden of Disease Study 2010, Lancet 380 (9859) (2012) 2095–2128.

[2] C.J.L. Murray, et al., Disability-adjusted life years (DALYs) for 291 diseases and injuries in 21 regions, 1990–2010: A systematic analysis for the Global Burden of Disease Study 2010, Lancet 380 (9859) (2012) 2197–2223.

[3] J. Bamford, P. Sandercock, M. Dennis, C. Warlow, J. Burn, Classification and natural history of clinically identifiable subtypes of cerebral infarction, Lancet 337 (8756) (1991) 1521–1526.

[4] S.C. Cramer, Repairing the human brain after stroke: I. Mechanisms of spontaneous recovery, Ann. Neurol. 63 (3) (2008) 272–287.

[5] A.K. Rehme, S.B. Eickhoff, L.E. Wang, G.R. Fink, C. Grefkes, Dynamic causal modeling of cortical activity from the acute to the chronic stage after stroke, Neuroimage 55 (3) (2011) 1147–1158.

[6] K. Arai, G. Jin, D. Navaratna, E.H. Lo, Brain angiogenesis in developmental and pathological processes: Neurovascular injury and angiogenic recovery after stroke, FEBS J. 276 (17) (2009) 4644–4652.

[7] K. Itoh, T. Maki, J. Lok, K. Arai, Mechanisms of cell-cell interaction in oligodendrogenesis and remyelination after stroke, Brain Res. 1623 (2015) 135–149, https://doi.org/10.1016/j.brainres.2015.04.039.

[8] M.A. Moskowitz, E.H. Lo, C. Iadecola, Review The Science of Stroke : Mechanisms in Search of Treatments, Neuron 67 (2) (2010) 181–198, https://doi.org/10.1016/j.neuron.2010.07.002.

[9] D. Leys, H. Hénon, M.-A. Mackowiak-Cordoliani, F. Pasquier, Poststroke dementia, Lancet Neurol. 4 (11) (2005) 752–759.

[10] J.B. Pinkston, N. Alekseeva, E.G. Toledo, Stroke and dementia, Neurol. Res. 31 (8) (2009) 824–831, https://doi.org/10.1179/016164109X12445505689643.

[11] L. Pantoni, Cerebral small vessel disease: from pathogenesis and clinical characteristics to therapeutic challenges, Lancet Neurol. 9 (7) (2010) 689–701.

[12] A. Joutel, F.M. Faraci, Cerebral small vessel disease: insights and opportunities from mouse models of collagen IV-related small vessel disease and cerebral autosomal dominant arteriopathy with subcortical infarcts and leukoencephalopathy, Stroke 45 (4) (2014) 1215–1221, https://doi.org/10.1161/STROKEAHA.113.002878.

[13] D.M. McTigue, R.B. Tripathi, The life, death, and replacement of oligodendrocytes in the adult CNS, J. Neurochem. 107 (1) (2008) 1–19, https://doi.org/10.1111/j.1471-4159.2008.05570.x.

[14] D.M. McTigue, R.B. Tripathi, The life, death, and replacement of oligodendrocytes in the adult CNS, J. Neurochem. 107 (1) (2008) 1–19, https://doi.org/10.1111/j.1471-4159.2008.05570.x.

[15] B. Menn, J.M. Garcia-Verdugo, C. Yaschine, O. Gonzalez-Perez, D. Rowitch, A. Alvarez-Buylla, Origin of oligodendrocytes in the subventricular zone of the adult brain, J. Neurosci. 26 (30) (2006) 7907–7918, https://doi.org/10.1523/JNEUROSCI.1299-06.2006.

[16] D.A. Greenberg, K. Jin, Growth Factors and Stroke, NeuroRx 3 (4) (2006) 458–465, https://doi.org/10.1016/j.nurx.2006.08.003.

[17] G. Mifsud, C. Zammit, R. Muscat, G. di Giovanni, M. Valentino, Oligodendrocyte Pathophysiology and Treatment Strategies in Cerebral Ischemia, CNS Neurosci. Ther. 20 (7) (2014) 603–612, https://doi.org/10.1111/cns.12263.

[18] M.A. Marin, S.T. Carmichael, Mechanisms of demyelination and remyelination in the young and aged brain following white matter stroke, Neurobiol. Dis. 126 (2019) 5–12.

[19] J.M. Garcia-verdugo, C. Yaschine, O. Gonzalez-perez, D. Rowitch, A. Alvarez-buylla, Origin of Oligodendrocytes in the Subventricular Zone of the adult brain, J. Neurosci. 26 (30) (2006) 7907–7918, https://doi.org/10.1523/JNEUROSCI.1299-06.2006.

[20] T. Maki, A.C. Liang, N. Miyamoto, E.H. Lo, K. Arai, Mechanisms of oligodendrocyte regeneration from ventricular-subventricular zone-derived progenitor cells in white matter diseases, Front. Cell. Neurosci. 7 (DEC) (2013), https://doi.org/10.3389/fncel.2013.00275.

[21] D. Dewar, S.M. Underhill, M.P. Goldberg, Oligodendrocytes and Ischemic Brain Injury, J. Cereb. Blood Flow Metab. 23 (3) (2003) 263–274.

[22] R. Zhang, M. Chopp, Z.G. Zhang, Oligodendrogenesis after cerebral ischemia, Front. Cell. Neurosci. OCT (2013), https://doi.org/10.3389/fncel.2013.00201.

[23] S.A. Back, C.D. Kroenke, L.S. Sherman, G. Lawrence, X.i. Gong, E.N. Taber, J. A. Sonnen, E.B. Larson, T.J. Montine, White matter lesions defined by diffusion tensor imaging in older adults, Ann. Neurol. 70 (3) (2011) 465–476.

[24] C. Collins, J.M. Rommens, D. Kowbel, T. Godfrey, M. Tanner, S.-i. Hwang, D. Polikoff, G. Nonet, J. Cochran, K. Myambo, K.E. Jay, J. Froula, T. Cloutier, W.-L. Kuo, P. Yaswen, S. Dairkee, J. Giovanola, G.B. Hutchinson, J. Isola, O.-P. Kallioniemi, M. Palazzolo, C. Martin, C. Ericsson, D. Pinkel, D. Albertson, W.-B. Li, J.W. Gray, Positional cloning of ZNF217 and NABC1: Genes amplified at 20q13.2 and overexpressed in breast carcinoma, PNAS 95 (15) (1998) 8703–8708.

[25] Y.e. Zhang, K. Chen, S.A. Sloan, M.L. Bennett, A.R. Scholze, S. O'Keeffe, H. P. Phatnani, P. Guarnieri, C. Caneda, N. Ruderisch, S. Deng, S.A. Liddelow, C. Zhang, R. Daneman, T. Maniatis, B.A. Barres, J.Q. Wu, An RNA-sequencing transcriptome and splicing database of glia, neurons, and vascular cells of the cerebral cortex, J. Neurosci. 34 (36) (2014) 11929–11947.

[26] T. Ishimoto, K. Ninomiya, R. Inoue, M. Koike, Y. Uchiyama, H. Mori, Mice lacking BCAS1, a novel myelin-associated protein, display hypomyelination, schizophrenia-like abnormal behaviors, and upregulation of inflammatory genes in the brain, Glia 65 (5) (2017) 727–739, https://doi.org/10.1002/glia.23129.

[27] K. Ninomiya, T. Ishimoto, T. Taguchi, Subcellular localization of PMES-2 proteins regulated by their two cytoskeleton-associated domains, Cell. Mol. Neurobiol. 25 (5) (2005) 899–911, https://doi.org/10.1007/s10571-005-4955-5.

[28] M.K. Fard, F. van der Meer, P. Sánchez, L. Cantuti-Castelvetri, S. Mandad, S. Jäkel, E.F. Fornasiero, S. Schmitt, M. Ehrlich, L. Starost, T. Kuhlmann, C. Sergiou, V. Schultz, C. Wrzos, W. Brück, H. Urlaub, L. Dimou, C. Stadelmann, M. Simons, BCAS1 expression defines a population of early myelinating oligodendrocytes in multiple sclerosis lesions, Sci. Transl. Med. 9 (419) (2017), https://doi.org/10.1126/scitranslmed.aam7816.

[29] D.A. Bennett, R.S. Wilson, D.W. Gilley, J.H. Fox, Clinical diagnosis of Binswanger's disease, J. Neurol. Neurosurg. Psychiatry 53 (11) (1990) 961–965.

[30] R.N. Kalaria, R.A. Kenny, C.G. Ballard, R. Perry, P. Ince, T. Polvikoski, Towards defining the neuropathological substrates of vascular dementia, J. Neurol. Sci. 226 (1–2) (2004) 75–80.

[31] S. Kaji, T. Maki, J. Ueda, T. Ishimoto, Y. Inoue, K. Yasuda, M. Sawamura, R. Hikawa, T. Ayaki, H. Yamakado, R. Takahashi, BCAS1-positive immature oligodendrocytes are affected by the α-synuclein-induced pathology of multiple system atrophy, Acta Neuropathol. Commun. 8 (1) (2020).

[32] L.M. Meservey, V.V. Topkar, M.-M. Fu, mRNA Transport and Local Translation in Glia, Trends Cell Biol. 31 (6) (2021) 419–423.

[33] S.C. Fagan, D.C. Hess, E.J. Hohnadel, D.M. Pollock, A. Ergul, Targets for Vascular Protection After Acute Ischemic Stroke, Stroke 35 (9) (2004) 2220–2225.

[34] Z.G. Zhang, L.i. Zhang, Q. Jiang, R. Zhang, K. Davies, C. Powers, N.V. Bruggen, M. Chopp, VEGF enhances angiogenesis and promotes blood-brain barrier leakage in the ischemic brain, J. Clin. Investig. 106 (7) (2000) 829–838.

[35] D.A. Greenberg, K. Jin, From angiogenesis to neuropathology, Nature 438 (7070) (2005) 954–959.

[36] H.-A. Abbaszadeh, T. Tiraihi, A. Delshad, M. Saghedizadeh, T. Taheri, H. Kazemi, H.K. Hassoun, Differentiation of neurosphere-derived rat neural stem cells into oligodendrocyte-like cells by repressing PDGF-α and Olig2 with triiodothyronine, Tissue Cell 46 (6) (2014) 462–469.

[37] I. K. Hart, W. D. Richardson, C. H. Heldin, B. Westermark, and M. C. Raff, "PDGF receptors on cells of the oligodendrocyte-type-2 astrocyte (O-2A) cell lineage," *Development*, vol. 105, no. 3, pp. 595–603, Mar. 1989, doi: 10.1242/dev.105.3.595.

[38] A. Cellerino, P. Carroll, H. Thoenen, Y.A. Barde, Reduced size of retinal ganglion cell axons and hypomyelination in mice lacking brain-derived neurotrophic factor, Mol. Cell. Neurosci. 9 (5–6) (1997) 397–408, https://doi.org/10.1006/mcne.1997.0641.

[39] Y.-P. Yan, K.A. Sailor, R. Vemuganti, R.J. Dempsey, Insulin-like growth factor-1 is an endogenous mediator of focal ischemia-induced neural progenitor proliferation, Eur. J. Neurosci. 24 (1) (2006) 45–54, https://doi.org/10.1111/j.1460-9568.2006.04872.x.

[40] J. Xiao, A.W. Wong, M.M. Willingham, M. van den Buuse, T.J. Kilpatrick, S. S. Murray, Brain-Derived Neurotrophic Factor Promotes Central Nervous System Myelination via a Direct Effect upon Oligodendrocytes, Neurosignals 18 (3) (2010) 186–202, https://doi.org/10.1159/000323170.

[41] B. Nait-Oumesmar, N. Picard-Riera, C. Kerninon, L. Decker, D. Seilhean, G. U. Höglinger, E.C. Hirsch, R. Reynolds, A. Baron-Van Evercooren, Activation of the subventricular zone in multiple sclerosis: Evidence for early glial progenitors, PNAS 104 (11) (2007) 4694–4699.

[42] G.L. Wang, B.H. Jiang, E.A. Rue, G.L. Semenza, Hypoxia-inducible factor 1 is a basic-helix-loop-helix-PAS heterodimer regulated by cellular O2 tension, PNAS 92 (12) (1995) 5510–5514, https://doi.org/10.1073/pnas.92.12.5510.

[43] R.K. Bruick, Oxygen sensing in the hypoxic response pathway: regulation of the hypoxia-inducible transcription factor, Genes Dev. 17 (21) (2003) 2614–2623.

[44] J.C. Chavez, F. Agani, P. Pichiule, J.C. LaManna, Expression of hypoxia-inducible factor-1α in the brain of rats during chronic hypoxia, J. Appl. Physiol. 89 (5) (2000) 1937–1942, https://doi.org/10.1152/jappl.2000.89.5.1937.

[45] O. Baranova, L.F. Miranda, P. Pichiule, I. Dragatsis, R.S. Johnson, J.C. Chavez, Neuron-specific inactivation of the hypoxia inducible factor 1α increases brain injury in a mouse model of transient focal cerebral ischemia, J. Neurosci. 27 (23) (2007) 6320–6332, https://doi.org/10.1523/JNEUROSCI.0449-07.2007.

[46] S.A. Back, B.H. Han, N.L. Luo, C.A. Chricton, S. Xanthoudakis, J. Tam, K.L. Arvin, D.M. Holtzman, Selective vulnerability of late oligodendrocyte progenitors to hypoxia-ischemia, J. Neurosci. 22 (2) (2002) 455–463.

[47] N. Miyamoto, T. Maki, A. Shindo, A.C. Liang, M. Maeda, N. Egawa, K. Itoh, E.K. Lo, J. Lok, M. Ihara, K. Arai, Astrocytes Promote Oligodendrogenesis after White Matter Damage via Brain-Derived Neurotrophic Factor, J. Neurosci. 35 (41) (2015) 14002–14008.

[48] Y. Béjot, A. Prigent-Tessier, C. Cachia, M. Giroud, C. Mossiat, N. Bertrand, P. Garnier, C. Marie, Time-dependent contribution of non neuronal cells to BDNF production after ischemic stroke in rats, Neurochem. Int. 58 (1) (2011) 102–111.

[49] Y. Béjot, C. Mossiat, M. Giroud, A. Prigent-Tessier, and C. Marie, "Circulating and Brain BDNF Levels in Stroke Rats. Relevance to Clinical Studies," *PLoS One*, vol. 6, no. 12, p. e29405, Dec. 2011, doi: 10.1371/journal.pone.0029405.

[50] S. Magami, N. Miyamoto, Y. Ueno, K. Hira, R. Tanaka, K. Yamashiro, H. Oishi, H. Arai, T. Urabe, N. Hattori, The Effects of Astrocyte and Oligodendrocyte Lineage Cell Interaction on White Matter Injury under Chronic Cerebral Hypoperfusion, Neuroscience 406 (2019) 167–175.
[51] G. Wolswijk, Chronic stage multiple sclerosis lesions contain a relatively quiescent population of oligodendrocyte precursor cells, J. Neurosci. 18 (2) (1998) 601–609, https://doi.org/10.1523/jneurosci.18-02-00601.1998.
[52] W. Jia, Y. Kamen, H. Pivonkova, R.T. Káradóttir, Neuronal activity-dependent myelin repair after stroke, Neurosci. Lett. 703 (February) (2019) 139–144, https://doi.org/10.1016/j.neulet.2019.03.005.
[53] B. Neumann, R. Baror, C. Zhao, M. Segel, S. Dietmann, K.S. Rawji, S. Foerster, C. R. McClain, K. Chalut, P. van Wijngaarden, R.J.M. Franklin, Metformin Restores CNS Remyelination Capacity by Rejuvenating Aged Stem Cells, Cell Stem Cell 25 (4) (2019) 473–485.e8.
[54] K. Psachoulia, F. Jamen, K.M. Young, W.D. Richardson, Cell cycle dynamics of NG2 cells in the postnatal and ageing brain, Neuron Glia Biol. 5 (3–4) (2009) 57–67, https://doi.org/10.1017/S1740925X09990354.
[55] E.C. Sams, Oligodendrocytes in the aging brain, Neuronal Signal 5 (3) (2021) 1–24, https://doi.org/10.1042/ns20210008.
[56] G.A. Rosenberg, Understanding aging effects on brain ischemia, Neurobiol. Dis. 126 (2019) 3–4, https://doi.org/10.1016/j.nbd.2019.04.002.

Supplementary Fig. 1

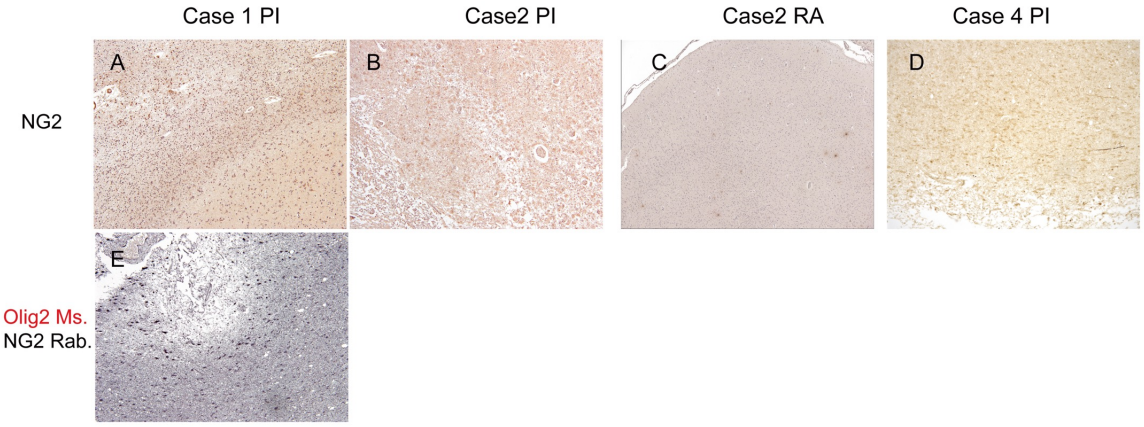

Supplementary Fig. 2

PI		Male (n=4)	Female(n=2)	P value
	PI-WM	273.5 ± 75.28 cells/mm²	293.5 ± 118.7 cells/mm²	>0.9999
	% PI-WM	46.76 ± 7.595%	48.14 ± 1.439%	0.5697
RA	RA	Male (n=4)	Female(n=2)	
	RA-cortex	79.23 ± 17.8 cells/mm²	50.71 ± 14 cells/mm²	0.3659
	RA-WM	185.1 ± 100.4 cells/mm²	49.44 ± 33.58 cells/mm²	0.5616
	%RA-cortex	64.82 ± 5.179%	59.37 ± 12.47%	0.8615
	% RA-WM	19.97 ± 12.22%	41.57 ± 22.97%	>0.9999
SVD	SVD	Male (n=4)	Female(n=4)	
	SVD-Cortex	17.75 ± 4.469 cells/mm²	24.53 ± 5.4 cells/mm²	0.2645
	SVD-WM	2.535 ± 0.6547 cells/mm²	13.52 ± 5.843 cells/mm²	0.3009
	%SVD-Cortex	73.98 ± 5.803%	68.26 ± 8.587%	0.7998
	%SVD-WM	12.43 ± 6.979%	22.85 ± 7.308%	0.1009
		Male (n=4)	Female(n=0)	
	PI-Cortex	159.4 ± 24.49cells/mm²	NA (*)	